JCB

Supplemental material

Watanabe et al., **https://doi.org/10.1083/jcb.201907006**

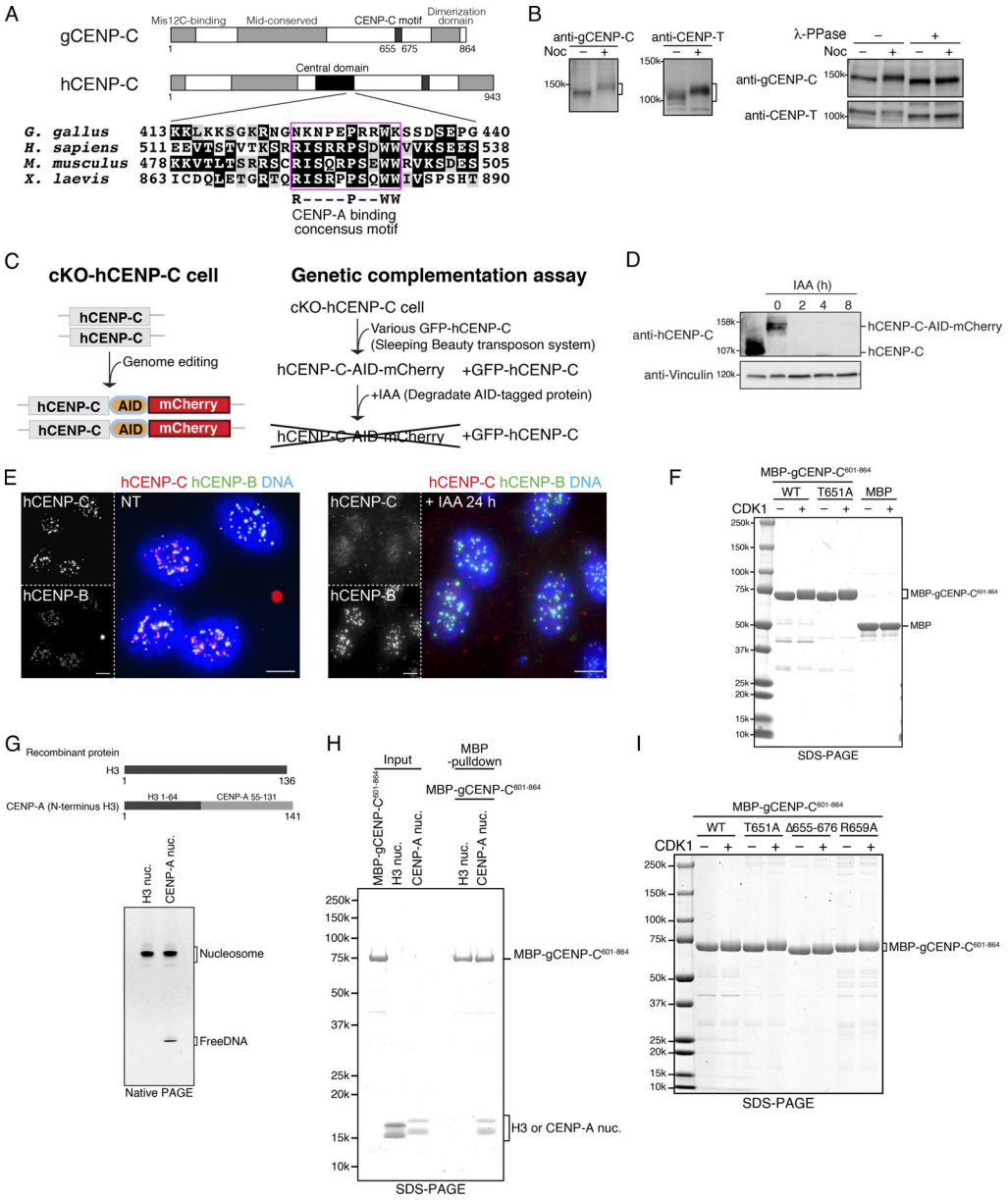

Figure S1. **gCENP-C phosphorylation, cKO-hCENP-C human RPE-1 cells, and recombinant proteins for the gCENP-C pull-down assay.** Related to Figs. 1 and 2. **(A)** Schematic representation of gCENP-C and hCENP-C. The lengths of chicken and hCENP-C are 864 and 943 aa, respectively. Alignment of partial CENP-C amino acid sequences. The magenta box shows the consensus motif of the central domain. **(B)** gCENP-C phosphorylation in mitotic arrested DT40 cells. Chicken DT40 cells were treated with or without nocodazole (Noc + or –) for 8 h. The cells were lysed and examined by immunoblotting (left panels). The cell lysates were treated with or without λ-phosphatase (λ-PPase + or –) and examined (right panels). **(C)** Schematic representation of AID-tag targeting to *hCENP-C* gene locus to generate a cKO-hCENP-C cell line (left). AID-tag sequence with *mCherry* gene was targeted into the *hCENP-C* gene locus in RPE-1 cells using TALEN. Using cKO-hCENP-C cells, genetic complementation was examined (right). **(D)** Degradation of hCENP-C fused with AID-mCherry in the presence of IAA. Parental RPE-1 cells are shown in the most left lane. The RPE-1 cells in which *AID-mCherry* was introduced into both *hCENP-C* alleles (cKO-hCENP-C human RPE-1 cells) were treated with IAA for the indicated time. hCENP-C fused with AID-mCherry (hCENP-C-AID-mCherry) was undetectable in the IAA-treated cells. Vinculin was probed as a loading control. **(E)** Localization of hCENP-C-AID-mCherry. The RPE-1 cells expressing hCENP-C-AID-mCherry (red) were treated with IAA for 24 h and then fixed and stained with an anti-human CENP-B (hCENP-B) antibody (green). DNA was stained with DAPI (blue). NT indicates cells not treated with IAA. Scale bars indicate 5 µm. **(F)** SDS-PAGE analysis for purified MBP-fused gCENP-C$^{601–864\ WT}$ (WT) and gCENP-C$^{601–864\ T651A}$ (T651A) phosphorylated or not by CDK1. MBP-gCENP-C$^{601–864}$ WT and T651A phosphorylated by CDK1 were examined by SDS-PAGE (CDK1+). MBP was used as a negative control. The same samples were used in Fig. 2 A. Nonphosphorylated proteins were also examined (CDK1–). **(G)** Native PAGE for in vitro re-constituted H3- and CENP-A–containing nucleosomes. Since chicken full-length CENP-A did not form stable nucleosomes using a salt dialysis method; therefore, we used the H3-CENP-A chimeric construct, which includes the centromere targeting domain (CATD) and C-terminal tail of CENP-A. H3 nuc. or CENP-A nuc. indicates nucleosomes containing a histone H3 or the H3-CENP-A chimeric construct, respectively. **(H)** Specific binding of gCENP-C$^{601–864}$ to CENP-A nucleosomes. The H3 or CENP-A nucleosome shown in G was mixed with MBP-fused gCENP-C$^{601–864\ WT}$ and pulled down by MBP. The CENP-A, but not H3, nucleosome bound to gCENP-C$^{601–864}$. **(I)** SDS-PAGE analyses of purified MBP-fused gCENP-C$^{601–864\ WT}$ and its mutants phosphorylated by CDK1. MBP-gCENP-C$^{601–864}$ WT, T651A, Δ655–676, and R659A phosphorylated by CDK1 shown in Fig. 2 D were examined by SDS-PAGE (CDK1+). Nonphosphorylated proteins were also examined (CDK1–).

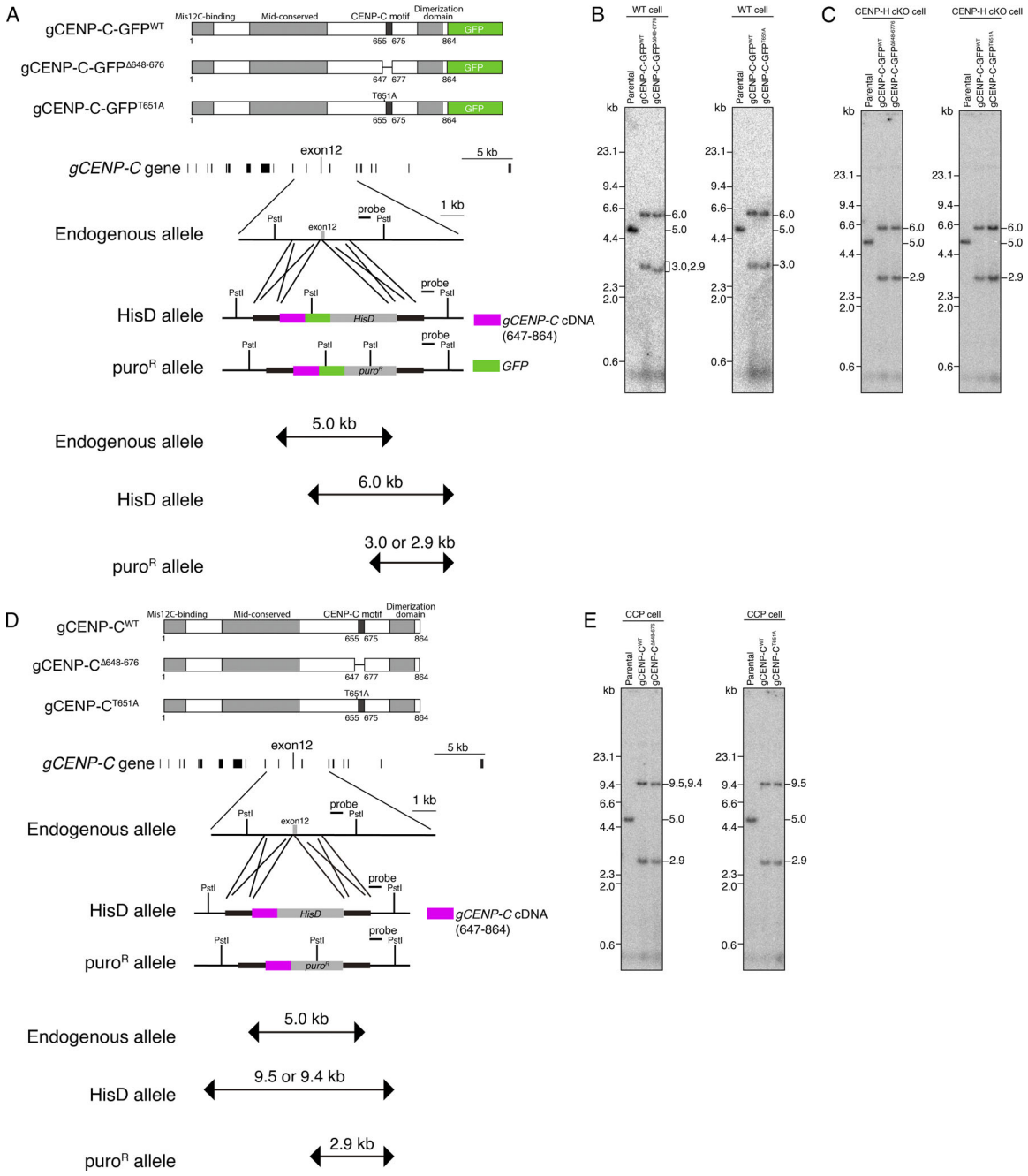

Figure S2. **Homologous recombination–mediated *gCENP-C* cDNA targeting into the endogenous *gCENP-C* genomic locus using the CRISPR/Cas9 system in DT40 cells.** Related to Figs. 3, 4, and 6. **(A)** Schematic representation of *GFP*-fused *gCENP-C* cDNA targeting into the endogenous *gCENP-C* genomic locus. To express GFP-fused gCENP-C (gCENP-C-GFP) WT or its CENP-C motif deletion or T651A mutant under control of the *gCENP-C* endogenous promoter, *gCENP-C* ORF cDNA covering exons 12–18 (coding aa 647–864) fused with GFP was targeted into exon 12 of the *gCENP-C* locus by CRISPR/Cas9-mediated homologous recombination. Since the targeting constructs have *HisD* (L-Histidinol resistance gene) or puromycin resistance genes (*puro*^{R}), targeted cells were selected using these selection markers. The indicated probe was used for Southern blot analysis shown in B and C. While the probe detects a 5.0-kb PstI-digested fragment for the endogenous allele, a 6.0-kb fragment was detected for the allele targeted with the cDNA construct with *HisD* (HisD allele). The allele targeted with the cDNA construct with *puro*^{R} (puro^R allele) results in 3.0- or 2.9-kb fragments following PstI digestion, because the 3′ homologous arm is longer in some constructs. **(B)** Southern blot analysis for genomic DNAs isolated from WT DT40 cells targeted with *gCENP-C* cDNA. Genomic DNA from each line was digested with PstI and analyzed by Southern hybridization using the probe as indicated in A. **(C)** Southern blot analysis of genomic DNAs isolated from CENP-H cKO (cKO-CENP-H) cells targeted with *gCENP-C* cDNA. Genomic DNAs from each line were digested with PstI and analyzed by Southern hybridization using the probe as indicated in A. **(D)** Schematic representation of *gCENP-C* cDNA targeting into the endogenous *gCENP-C* genomic locus. To express gCENP-C WT, its CENP-C motif deletion, or the T651A mutant under control of the *gCENP-C* endogenous promoter, the *gCENP-C* ORF cDNA as shown above, without GFP, was targeted into exon 12 of the *gCENP-C* locus, as shown in A. The probe for Southern blot analysis used in E detects 5.0- or 2.9-kb PstI digestion fragments for endogenous or *puro*^{R} alleles, respectively. The *HisD* allele results in a 9.5 kb fragment for WT and T651A cDNAs, and a 9.4-kb fragment for Δ648-676 cDNA. **(E)** Southern blot analysis of genomic DNA isolated from CCP cells targeted with the *gCENP-C* cDNA. Genomic DNA from each line was digested with PstI and analyzed by Southern hybridization with the probe as indicated in D.

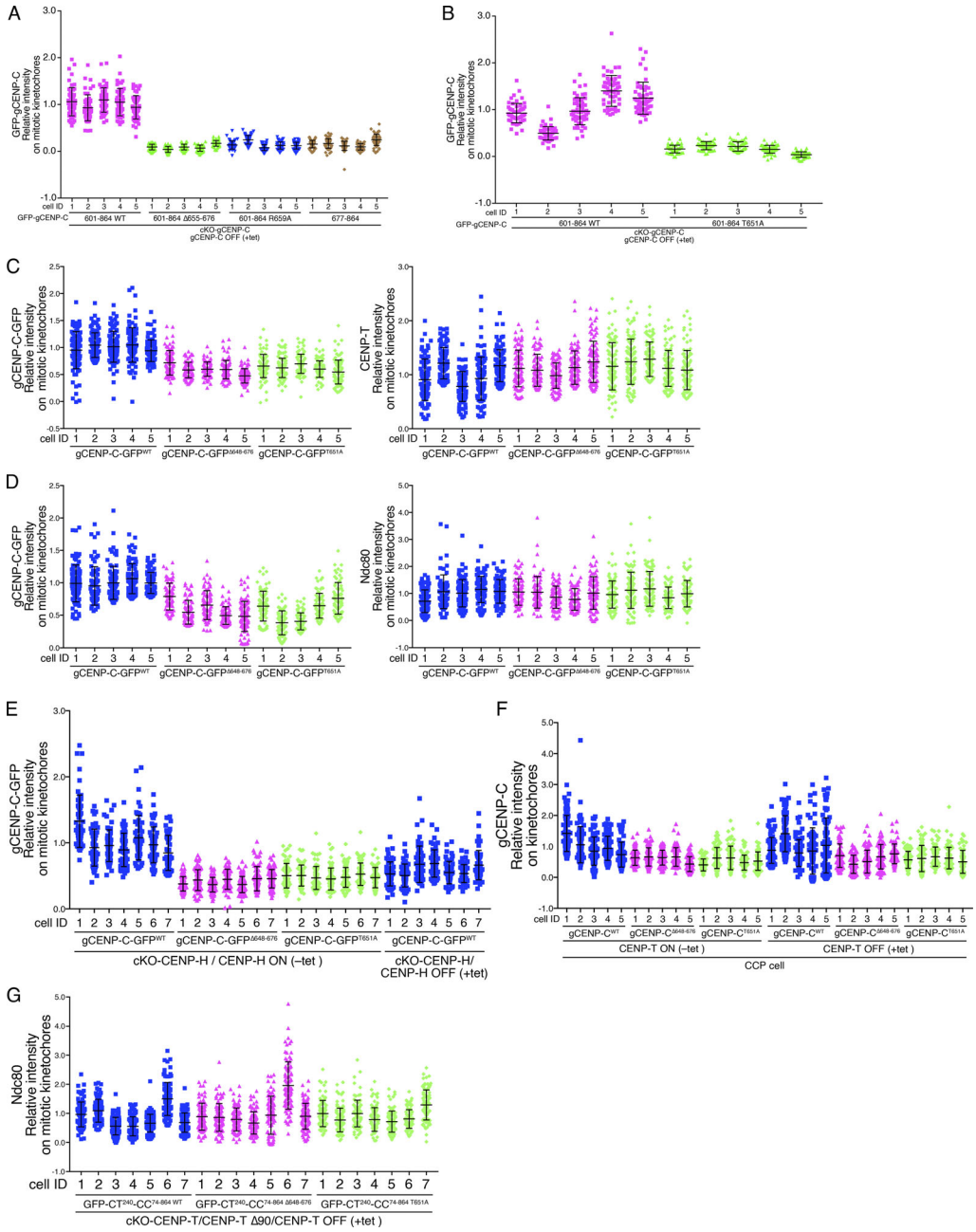

Figure S3. **Signal intensities of gCENP-C-GFP on mitotic kinetochores in gCENP-C-GFP knocked-in DT40 cell lines.** Related to Figs. 1, 3, 4, 6, and 7. **(A)** Signal intensities of various GFP-fused CENP-C C-terminal fragments on mitotic kinetochores in each clone of the cell lines shown in Fig. 1 D. The signal intensities of GFP on kinetochores in mitotic cells were quantified; >50 kinetochores for each of the five clones in each line were examined. Average of each clone for each line is presented in Fig. 1 D. **(B)** Signal intensities of GFP-fused gCENP-C$^{601–864}$ WT or T651A on mitotic kinetochores in each clone of the cell lines shown in Fig. 1 G. The signal intensities of GFP on kinetochores in mitotic cells were quantified; >50 kinetochores for each of five clones in each line were examined. Average of each clone for each line is presented in Fig. 1 G. **(C)** gCENP-C-GFP and CENP-T signal intensities on mitotic kinetochores in each clone of the cell lines shown in Fig. 3 B. The signal intensities of gCENP-C-GFP and CENP-T on kinetochores in mitotic cells were quantified; >80 kinetochores for each of five clones in each line were examined. Average of each clone for each line is presented in Fig. 3 B. **(D)** gCENP-C-GFP and Ndc80 signal intensities on mitotic kinetochores in each clone of the cell lines shown in Fig. 3 C. The signal intensities of gCENP-C-GFP and Ndc80 on kinetochores in mitotic cells were quantified; >70 kinetochores for each of five clones in each line were examined. Average of each clone for each line is presented in Fig. 3 C. **(E)** gCENP-C-GFP signal intensities on mitotic kinetochores in each clone of the cell lines shown in Fig. 4 B. The signal intensities of gCENP-C-GFP on mitotic kinetochores in the gCENP-C-GFP knocked-in cKO-CENP-H in the presence or absence of tet (+tet: CENP-H OFF or –tet: CENP-H ON) for 48 h were quantified; >50 kinetochores for each of seven clones in each line were examined. Average of each clone for each line is presented in Fig. 4 B. **(F)** CENP-C signal intensities on mitotic kinetochores in each clone of the CCP cell lines are shown in Fig. 6 D. The signal intensities of CENP-C on kinetochores in mitotic cells were quantified; >70 kinetochores for each of five clones in each line were examined. The average of each clone for each line is presented in Fig. 6 D. **(G)** Ndc80 signal intensities on mitotic kinetochores in each clone of the cKO-CENP-T/CENP-T Δ90 with expressing GFP-CT^{240}-CC$^{74–864}$ cell lines are shown in Fig. 7 E. The signal intensities of Ndc80 on kinetochores in mitotic cells were quantified; >80 kinetochores for each of seven clones in each line were examined. The average of each clone for each line is presented in Fig. 7 E. Error bars indicate SD.

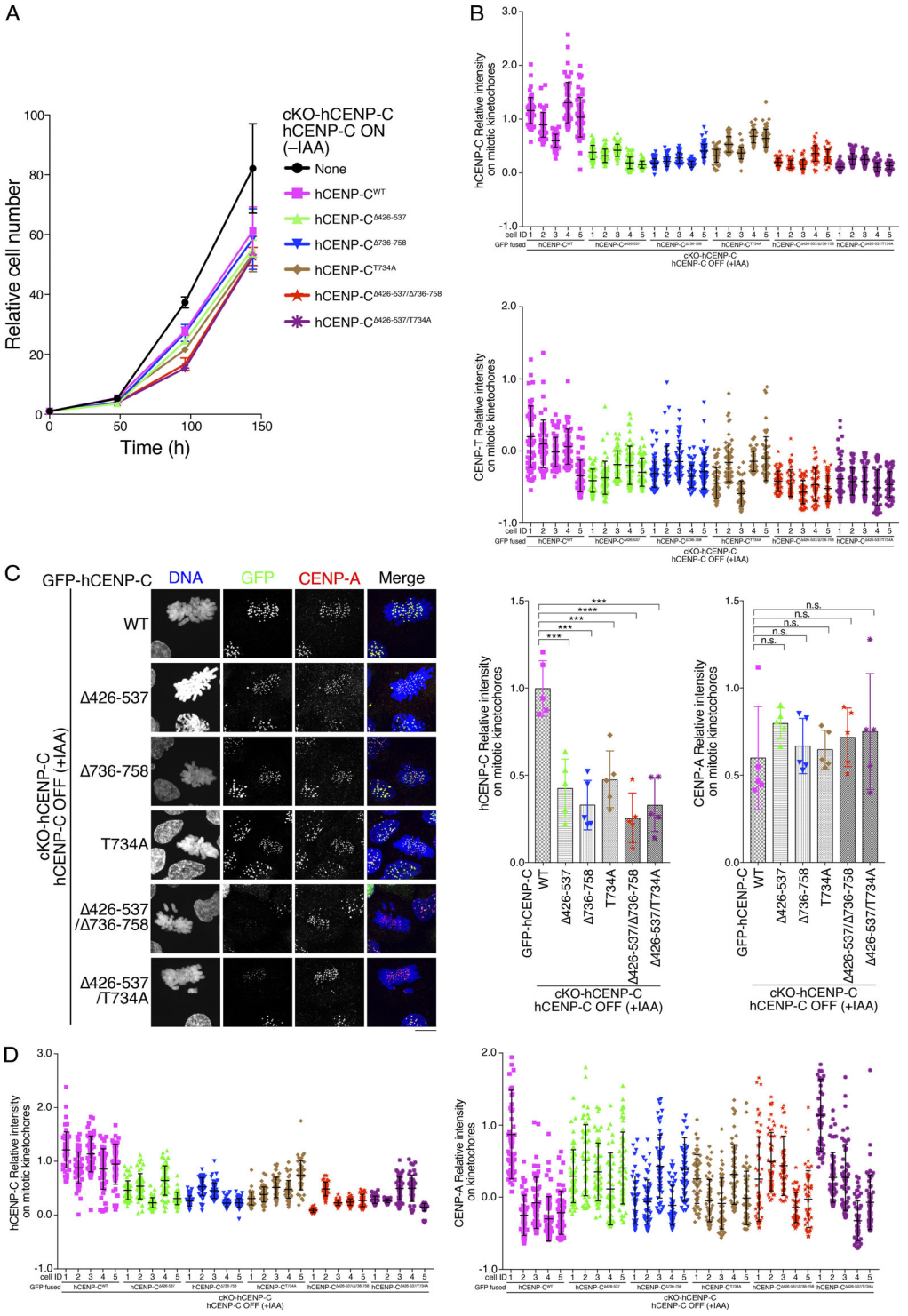

Figure S4. **Growth of cKO-hCENP-C RPE-1 cells expressing hCENP-C or its mutants in the absence of IAA and localization of mutant hCENP-C.** Related to Fig. 5. **(A)** Growth of cKO-hCENP-C human RPE-1 cells expressing GFP-fused hCENP-C WT, Δ426–537, Δ736–758, T734A, Δ426–537/Δ736–758, and Δ426–537/T734A in the absence of IAA. Parental cKO-hCENP-C human RPE-1 cells (None) were also examined. The presented graphs are mean results of three independent experiments. **(B)** GFP and CENP-T signal intensities on mitotic kinetochores in each clone of the cell lines shown in Fig. 5 E. More than 50 kinetochores for each of five clones in each line were examined. Average of each clone for each line is presented in Fig. 5 E. **(C)** Localization of CENP-A in cKO-hCENP-C human RPE-1 expressing GFP-fused hCENP-C WT or its mutants. GFP-hCENP-C localization was examined in the cells after IAA addition (green). CENP-A was stained with an anti-CENP-A antibody (red). DNA was stained by DAPI (blue). Scale bar indicates 10 µm. The signal intensities of GFP and CENP-A on the mitotic kinetochores in each cell line treated with IAA were quantified. Bar graph indicates mean with SD (n = 5; ****, P < 0.0001; ***, P < 0.001; NS, P > 0.05, unpaired t test, two tailed). **(D)** Signal intensities of various GFP-fused hCENP-C and CENP-A on mitotic kinetochores in each clone of the cell lines shown in C. More than 50 kinetochores for each of five clones in each line were examined. Average of each clone for each line is presented in graph of C. Error bars indicate SD.

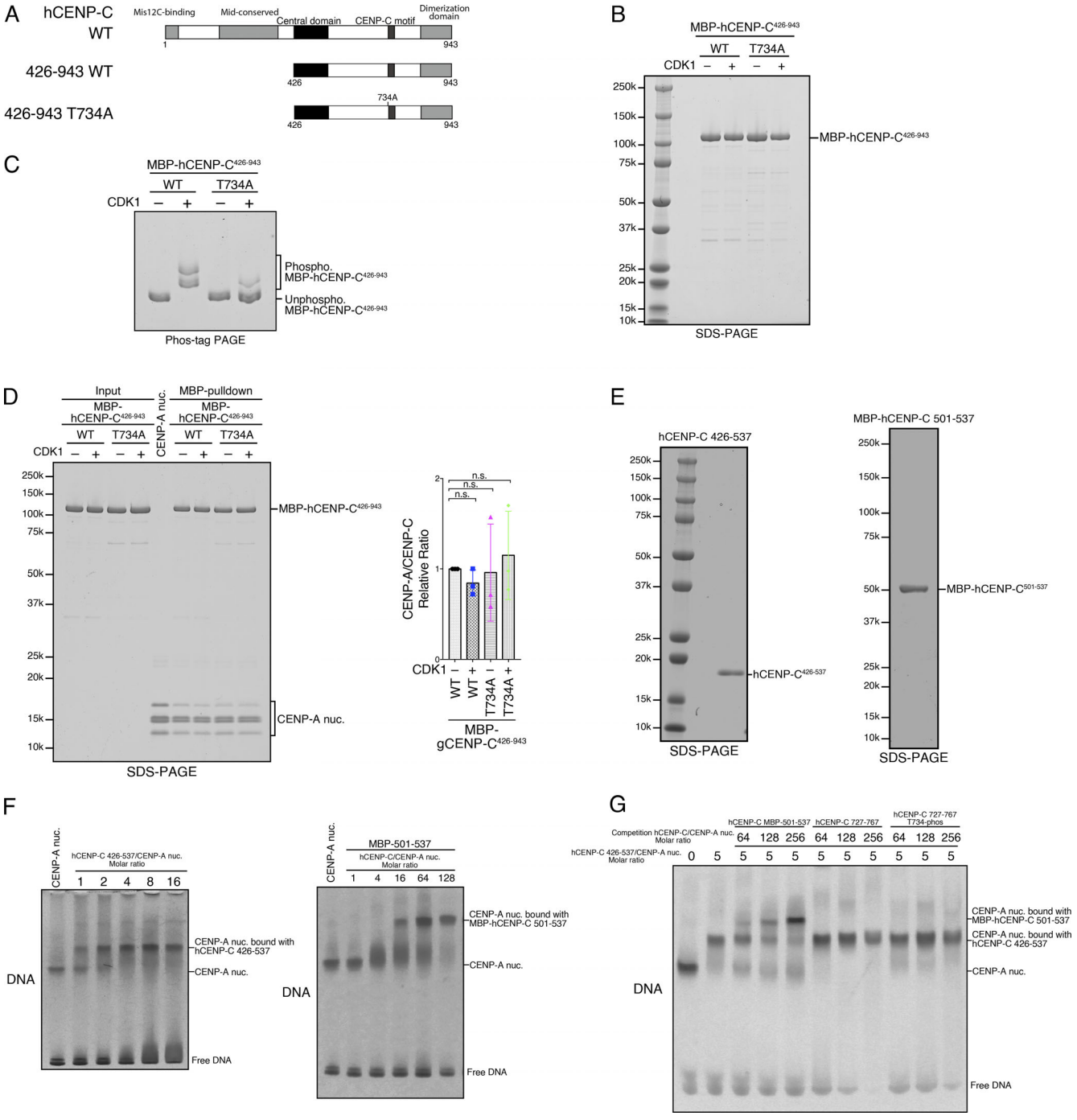

Figure S5. **Biochemical analyses using the hCENP-C C-terminal fragment.** Related to Fig. 5. **(A)** Schematic representation of full-length WT hCENP-C (WT) and its derivatives (426–943 WT and 426–943 T734A). **(B)** SDS-PAGE analysis for purified MBP-fused hCENP-C$^{426–943}$ WT and T734A phosphorylated by CDK1 (CDK1+). Nonphosphorylated proteins were also examined (CDK1–). **(C)** Phos-tag PAGE analysis for purified MBP fused to hCENP-C$^{426–943\ WT}$ and hCENP-C$^{426–943\ T734A}$ phosphorylated by CDK1 (CDK1+). Unphosphorylated proteins (CDK1–) were also examined. **(D)** MBP pull-down for the CENP-A nucleosome with MBP-hCENP-C$^{426–943}$ WT and T734A phosphorylated or unphosphorylated by CDK1. Signal intensities of all histones in CENP-A nucleosomes precipitated with MBP proteins were quantified as pulled down CENP-A nucleosomes. The presented data are mean results of three independent experiments. **(E)** SDS-PAGE analysis of purified hCENP-C$^{426–537}$ and MBP-fused hCENP-C$^{501–537}$. **(F)** Native PAGE analysis of the human CENP-A nucleosome complex with hCENP-C$^{426–537}$ or MBP-hCENP-C$^{501–537}$. The nucleosome and CENP-C–nucleosome complex were visualized by staining DNA bound to them with ethidium bromide. The CENP-A–CENP-C complex migrated more slowly than the CENP-A nucleosome. Molar ratios of added CENP-C proteins to the CENP-A nucleosome are shown. **(G)** A competition assay of the CENP-A nucleosome binding of hCENP-C$^{426–537}$ with MBP-hCENP-C$^{501–537}$or phosphorylated or unphosphorylated hCENP-C$^{727–767}$ peptide. Molar ratios of CENP-C peptides added to the CENP-A nucleosome are shown. While excess MBP-hCENP-C$^{501–537}$ outcompeted the CENP-A nucleosome bound with hCENP-C$^{426–537\ WT}$, neither phosphorylated nor unphosphorylated hCENP-C$^{727–767}$ peptide did, suggesting that MBP-hCENP-C$^{501–537}$ shows higher affinity to the CENP-A nucleosome than hCENP-C$^{727–767}$ peptide.